International Innovative Research Journal of Engineering and Technology
ISSN: 2456-1983 Vol: 5 Issue: 2 December 2019

Radiation Safety Criteria Use of Neural Intelligence Systems in Gamma Camera Electric Circuit Modeling

[1]Mohd Samsu Sajat, [2]Khuzairi Mohd Zaini
[1,2]School of Computing, Universiti Utara Malaysia, 06010 UUM Sintok, Kedah, Malaysia

Abstract: This study was undertaken by using neural intelligence systems integrated with Gamma camera electrical circuit (DICOM – MATLAB integration systems) to evaluate radiation safety criteria during the nuclear imaging process with Gamma camera. In this research, we used the 40 uCi of Tc-99 m point source for gamma camera calibration, as well as thallium activated sodium iodide (NaI (Tl) crystal as radiation detector, which is presented throughout gamma camera by a variety of photomultiplier tubes (PMTs). In this analysis, we are using A Jaczack phantom with 6 fillable sphere for image processing under minimal effect of low doses with calibrated. The characteristic factor ratio was measured against standard gamma camera machine ratio, standardized uptake value (SUV), point spread function (PSF), signal-to-noise ratios (SNRs) were measured in accordance with the NEMA standard. SUV max, also PSF and SNRs for image reconstruction using DICOM – MATLAB achieved high-quality image reconstruction under low-dose Tc-99 m radio isotope circumstances. On the other hand, data revealed during the operating system process with DICOM- MATLAB system, high-quality image and low-dose, short exposure time and all radiation safety criteria were achieved under nuclear imaging radiation safety requirements.

Keywords: protection of radiation; neural intelligence systems; gamma camera; electrical circuit; DICOM – MATLAB; uniform uptake value; point-to-noise ratios; national association of electrical manufacturers;

1. INTRODUCTION

The radiation protection requirements on justification of a practice, dose limitation and optimization of protection, and the use of dose constraints apply to radiotherapy and radio and nuclear imaging. Radiation safety criteria principles as applied to occupational and public exposure as well as medical exposure. Dose limits refer to clinical exposure and are important for potential exposure control [1]. Most 99mTc diagnostic procedures for gamma camera machines need radiation safety standards justifications. With reference to the BSS series of safety reports No. 40 [2]. Throughout the use of facilities, the nuclear medicine equipment and the associated auxiliaries and instruments must meet all acceptability criteria [3]. Artificial Intelligence has proved to produce promising results where incomplete, unclear or skewed data are available in digital image processing and analysis. Decision support systems, neural networks, DICOM systems and MATLAB systems are capable of coping with ambiguous, uncertain, conflicting, complementary, imprecise and redundant data, such as that which occurs in the field of biomedical imaging, to provide a more reliable and less uncertain interpretation [4, 5]. The process of transforming different data sets into one coordinate system is the registration of images. Registration is necessary in order to allow the correlation, integration and fusion of images from different measurements that can be taken from the same modality at different times or obtained from the different modalities in the gamma camera [6, 7]. It is also possible to use non-stiff registration of medical images to record the data of a patient in an anatomical atlas [8]. Registration of medical images is a pre-processing step for many medical imaging applications and may have a strong impact on the result of subsequent segmentation and edge detection [9,10]. Such artificial intelligence facilities have the power to support performance imaging and can also be considered as one of the technological security standards during the processes of nuclear imaging [11, 12]. An electrical design with a preamplifier circuit coupled to synchronization with a gamma camera scintillator will be built to simulate another slightly different form signal by simply adjusting a few parameter values [13, 14]. The developed design such as DICOM can boost the quality performance of electrical circuit control in gamma camera scintillator, as well as the DICOM and neural intelligence systems function as a power to improve the PMT photocathode's quantum efficiency [15].

2. AIM

We need to use all facilities during the processing of radiation safety for gamma camera equipment to improve and support the radiation safety systems during diagnosis with nuclear imaging. The goal of this study is to use the DICOM- MATLAB Neural Intelligence Systems (NIS) collaborated with electrical gamma camera circuits during the imaging process, which resulted in improved image quality imaging, image recovery, image restoration (including de-noise and enhancement) – short time for exposure to radiation, low doses for radio isotopes during radio diagnosis. The previous technical criteria were established during the nuclear imaging process as technical radiation safety criteria [16].

3. MATERIALS AND METHODS

The gamma camera system and accessories mounted at Moscow University Hospital's Nuclear Medicine Institute, Moscow (Russia) consisted of a thin but large-scale thallium activated sodium iodide (NaI(Tl)) crystal as a radiation detector seen by a series of photomultiplier tubes (PMTs). This NaI(Tl) crystal thickness camera is completely digital in the sense that an analog-to-digital converter (ADC) digitizes the output of each photomultiplier tube directly. Based on the recommendations of the National Electrical Manufacturers Association (NEMA) [17], in standardized experimental protocol for measuring gamma camera performance, The handheld gamma camera consists of a thick hexagonal parallel hole collimator with 1.3 mm hole size and 0.2 mm septa (5) coupled to a 2929 pixelated NaI (Tl) scintillation crystal array with an individual crystal size and 1.7 mm pitch coupled to a flat panel, multi-anode Hamamatsu H8500 Position Sensitive Photomultiplier (PSPMT) [18].

4. TECHNIQUES AND METHODS

Get about 40uCi of Tc-99 m in a point source configuration (activity is acceptable in an ICC volume or less). Carefully test the source, recording the activity and the calibration time in a calibrated dose calibrator. Suspend the origin from the detector and on the central axis of the detector at least five crystal diameters. Carefully measure the distance and record. Center the photo peak in a window of 15% or 20%, based on the clinical use. (Most manufacturers ' specifications have a 20% window). The slit was positioned at a slight angle directly on the entry window of the camera (slant ratio ~4-8). A Tc-99 m point source was mounted at a distance of ~ 1 meter directly above the slit so that the detector layer was flooded uniformly. The intrinsic uniformity of the system was calculated and the integral and differential uniformity were measured according to (NEMA, 2001) [19] for standardized uptake value (SUV), point spread function (PSF), signal-to-noise ratios (SNRs). The slit was slightly bent with regard to the array's pixel columns so that the line input dropped with regard to the crystal centers at different locations. Subsequently, profiles were obtained along the slit image distance. Intrinsic air count rate performance: a source of 99mTc radiation with 25mCi activity was used. Using the Copper sheet attenuation method, counts for a preset time of 20 sec were acquired using a 128 average 128 matrix size. Energy intrinsic resolution: a point source of 99mTc has been used. At a preset count, an image was acquired using a 1024 x 1024 pixel matrix size. A Jaszczak phantom was used in the study with 6 fillable spheres The Jaszczak cylindrical phantom weighed 8.3 kg and developed polymethylmethacrylate content with 9.89, 12.43, 15.43, 19.79, 24.82 and 31.27 mm internal diameter hot spheres. Events are connected to individual crystals and plotted as a function of the location of the known source. The resulting trapezoid response function's FWHM specifies the array's intrinsic spatial resolution. The counts in neighboring crystals show inter-crystal scattering, light diffusion, and unrelated background events Figure 1[20].

5. RESULTS AND DISCUSSION

Table 1 showed SUV before DICOM and MATLAB were analyzed. The SUV1 to SUV6 accounted for 6.95%, 6.93%, 5.69%, 5.01, 4.33% and 2.9% respectively. On the other hand, the high mean ratio of SUV type 1 to 6 was estimated at 8.21%, 8.13%, 7.75%, 6.85%, 5.97% and 4.35% respectively. Until processing with DICOM and MATLAB, 16.82, 15.36, 14.27, 9.88, 5.75 and 3.28 mm were also shown in Table 1 and Figure 2A-C. On the other hand, SUV sphere diameter reported with higher diameter than SUV before processing with DICOM and MATLAB after processing with DICOM and MATLAB. The previous research were associated with Hinton [21], where statistical models such as support vector machines, multivariate logistic regression, and artificial neural networks imply high accuracy object reconstructions. Table 2 shows the results of the Point Spread Function (PSF). 22.35 percent, 20.63, 18.69, 16.54, 14.75 and 11.82 percent were recorded before processing with DICOM and MATLAB. On the other hand, after processing with DICOM and MATLAB, the PSF ratio reported a high mean ratio of 33.25%, 28.64, 25.47,

International Innovative Research Journal of Engineering and Technology
ISSN: 2456-1983 Vol: 5 Issue: 2 December 2019

24.86, 20.14 and 16.28% respectively. The PSF – DICOM and MATLAB sphere diameter registered the highest level without DICOM and MATLAB, where 18.22 mm, 16.35, 13.47, 10.89, 7.96, 5.46 mm, respectively, were reported. Figure 3A-C showed image reconstruction after and before the processing of DICOM-MATLAB. In order to obtain good image quality at low doses from radioisotope compounds, the improved PSF component parallel to the SUV factor resulted in a decrease in exposure time during Gamma Camera image processing.

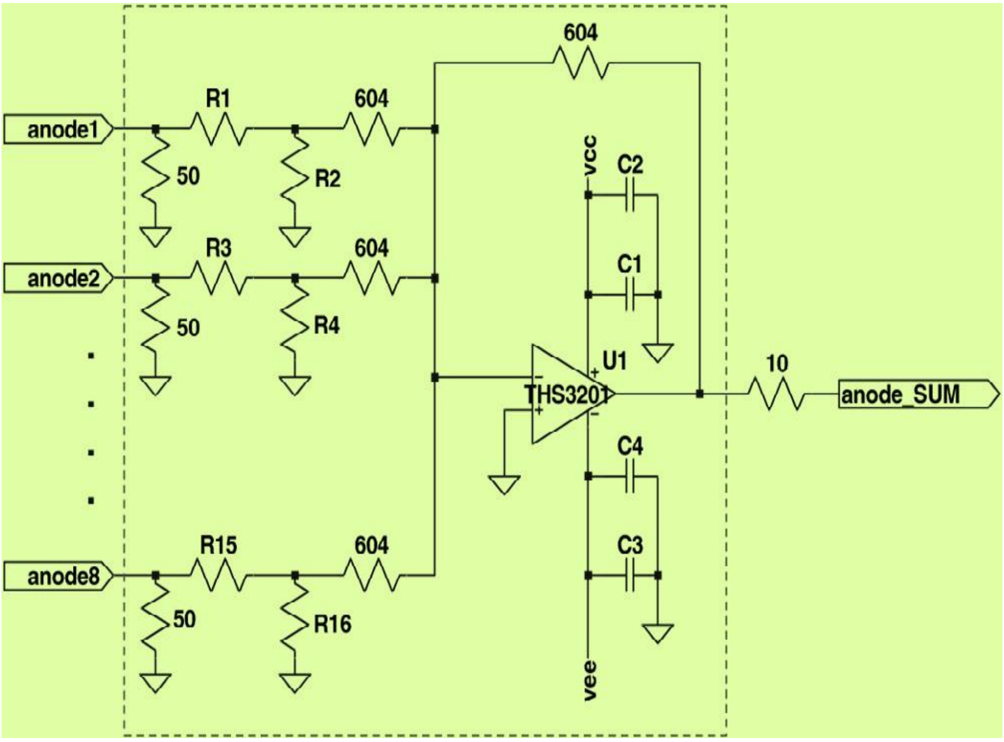

Figure 1. Electrical circuit schematics used to conduct the anode summing circuit in the front-end electronics for Gamma camera reading from the multi-anode PMT

Table 1. Standardized uptake value SUV ratio before and after processing with DICOM Resolution neural network and MATLAB resolution

Before processing with DICOM			After processing with DICOM and MATLAB			
SUV NO	SUV Mean Ratio%	Sphere Diameter/mm	SUV Mean Ratio%	Sphere Diameter/ mm	DICOM resolution Ratio %	MATLAB resolution Ratio %
SUV1	6.95	16.82	8.21	24.90	13.67	8.90
SUV2	6.93	15.36	8.13	19.50	13.53	10.55
SUV3	5.69	14.27	7.75	16.00	10.75	8.24
SUV4	5.01	9.88	6.85	11.00	6.45	5.06
SUV5	4.33	5.75	5.97	8.60	5.14	3.79
SUV6	2.9	3.28	4.35	7.40	5.05	3.74

International Innovative Research Journal of Engineering and Technology
ISSN: 2456-1983 Vol: 5 Issue: 2 December 2019

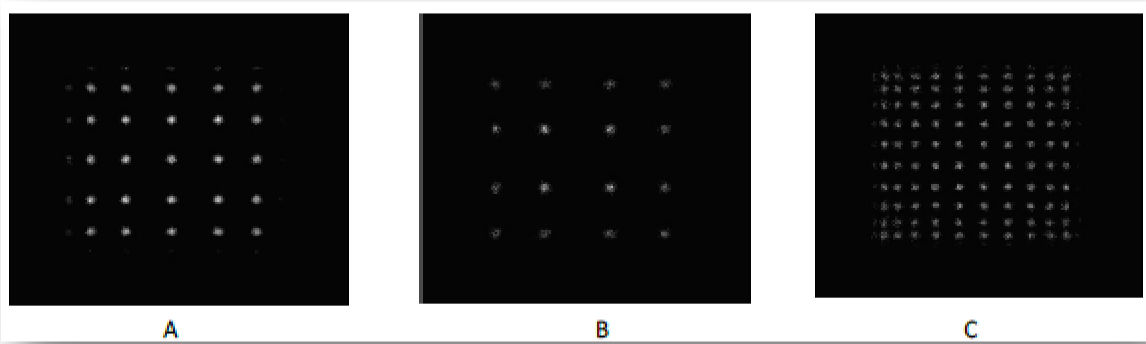

Figure 2. (A and B) The image reconstruction of SUV before processing with DICOM, (C) Image reconstruction after processing with DICOM

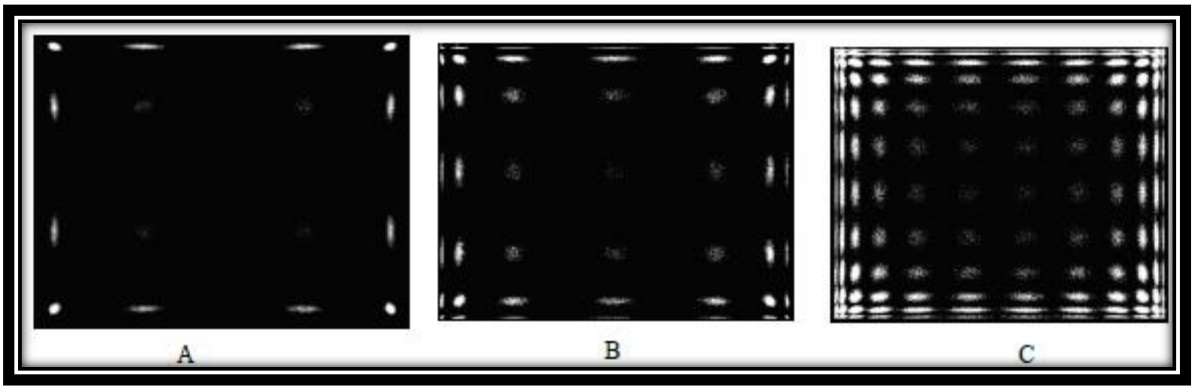

Figure 3. (A and B) The image reconstruction of PSF before processing with DICOM, (C) Image reconstruction after processing with DICOM

Gamma Camera's picture measurement reliability is influenced by the measuring equipment values for PSF and SUV action levels [22]. Gamma Camera manufacturers should use DICOM – MATLAB development systems to incorporate the quality assurance framework for PSF and SUV [23]. Such quality and assurance requirements are defined in the Nuclear Medicine's amended guideline on radiological protection [24]. During the imaging process with Gamma Camera [24], this analysis and description of specific action rates assisted sensitivity limits for radioisotopes. During the imaging process with Gamma Camera [24], this analysis and description of specific action rates assisted sensitivity limits for radioisotopes. Signal-to-noise ratio (SNR) findings are reported in Table 3. For DICOM and MATLAB 42.33 %, 39.25%, 36.37 %, 33.68 %, 31.97 % and 28.58 % respectively, SNRs mean ratio before DICOM and MATLAB processing reported higher levels than SNRs. On the other hand, DICOM reported 8.21 % of SNRs, 8.13, 7.75, 6.85, 5.97 and 4.35 % of SNRs. Of SNRs with DICOM sphere diameter reported lower than SNRs without DICOM – MATLAB systems 3.44 mm, 2.88 mm, 2.63 mm, 2.32 mm, 1.22 mm and 1.18 mm respectively. At 40 uCi of Tc-99 m, the resolution ratio for image reconstruction with DICOM-MATLAB in Gamma Camera registered a high SNR ratio of 1 to 6 (88.36 %, 64.36 %), (62.55%, 58.74 %), (85.33 %, 58.74 %), (78.96 %, 55.18), (72.82 %, 54.38%) and (71.35%, 52.48 %) respectively. Figure 4A-C, shown after and before DICOM-MATLAB processing simulated object reconstruction. This evidence are consistent with Groch 2001[26], which indicates that factors affecting silicon photomultiplier noise include dark counts after pulse and optical cross-discussion. In the bulk or surface depleted region at the junction, thermally produced electron hole pairs produce a leakage current that results in dark counts at PMT in Gamma camera during the nuclear imaging process. As a consequence of surface leakage current for electrical circuit [27], the contribution of dark current below breakdown voltage increases linearly with the bias voltage. In this analysis, several variables were influenced during the processing of imagery with Gamma

International Innovative Research Journal of Engineering and Technology
ISSN: 2456-1983 Vol: 5 Issue: 2 December 2019

camera on radiation safety criteria and achieved optimum quality assurance. Several associations and parallel variables should be taken into consideration during nuclear imaging for the radiation safety norm. The results showed relationships between SUV and PSF iteration number in Figures 5 and 6, showing the high-level ratio of SUV and PSF in PSF 9 iteration and PSF iteration 6 iteration. These findings have led to DICOM – MATLAB processing during Gamma camera scanning, while Gamma camera technology has been improved from basic electrical network circuits and integrated neural network intelligence systems [28]. In the development of the gamma camera detector, there are many factors to be considered. A small gamma camera field of view will be used as a prototype for a large area detector. Ideally, though remaining cost-effective, our imaging system would have high energy and spatial resolution. The detector's intrinsic spatial resolution increases as the size of segmented crystals decreases [29]. Figure 7 shows the results of the relationship between SUV (Standardized Uptake Value) and image sphere diameter at standard Gamma camera value machine without DICOM – MATLAB device processing. At the standard sphere diameter of 12.6 mm, the SUV max reported a high ratio of 11 mm sphere diameter with 27.5 percent. On the other hand, the effects of the relationship between sphere diameter and SNRs (single to noise ratios) and picture sphere diameter at 3 and 6 and 9 regulations are shown in Figures 8 and 9. The standard sphere diameter of 2 mm had a high-level ratio of 20.5 percent with 9 regulations. By comparison, the normal sphere diameter of 12 mm was small with 3 regulations at 10.2%. The results of the relationship between SNRs (single-to-noise ratios) and PSF (point spread function) are shown in Figure 9. The PSF regulation 9 with a sphere diameter of 12 mm had a high ratio of 10.2% with SNRs. On the other hand, PSF regulation 2 recorded a moderate ratio of 6.8 percent with sphere diameter 12. Such findings are consistent with Muntean, 2017 [30], which indicates that in MATLAB – DICOM neural intelligence systems, the gamma camera was modeled using crystal geometries for reconstructed images and energy spectrums to determine optimum parameters.

Table 2. Point spread function (PSF) ratio before and after treated with DICOM Resolution neural network and MATLAB resolution

Before processing with DICOM			After processing with DICOM and MATLAB			
PSF NO	PSF Mean Ratio%	Sphere Diameter/mm	PSF Mean Ratio%	Sphere Diameter mm	DICOM resolution Ratio %	MATLAB resolution Ratio %
PSF1	22.35	10.33	33.25	18.22	66.78	72.68
PSF2	20.63	8.63	28.64	16.35	65.47	68.57
PSF3	18.69	9.66	25.47	13.47	62.71	66.94
PSF4	16.54	7.35	24.86	10.89	58.42	64.12
PSF5	14.75	4.22	20.14	7.96	54.34	62.38
PSF6	11.82	2.79	16.28	5.46	52.53	59.72

Table 3. Signal-to-noise ratios (SNRs) before and after treated with DICOM Resolution neural network and MATLAB resolution

Before processing with DICOM			After processing with DICOM and MATLAB			
SNRs NO	SNRs Ratio%	Mean	Sphere Diameter/mm	SNRs Mean Ratio%	Sphere Diameter mm	DICOM resolution Ratio %	MATLAB resolution Ratio %

International Innovative Research Journal of Engineering and Technology
ISSN: 2456-1983 Vol: 5 Issue: 2 December 2019

SNR1	42.33	6.22	8.21	3.44	88.36	64.36
SNR2	39.25	4.12	8.13	2.88	85.62	62.55
SNR3	36.37	3.64	7.75	2.63	85.33	58.74
SNR4	33.68	2.58	6.85	2.32	78.96	55.18
SNR5	31.97	2.12	5.97	1.22	72.82	54.38
SNR6	28.58	1.38	4.35	1.18	71.35	52.48

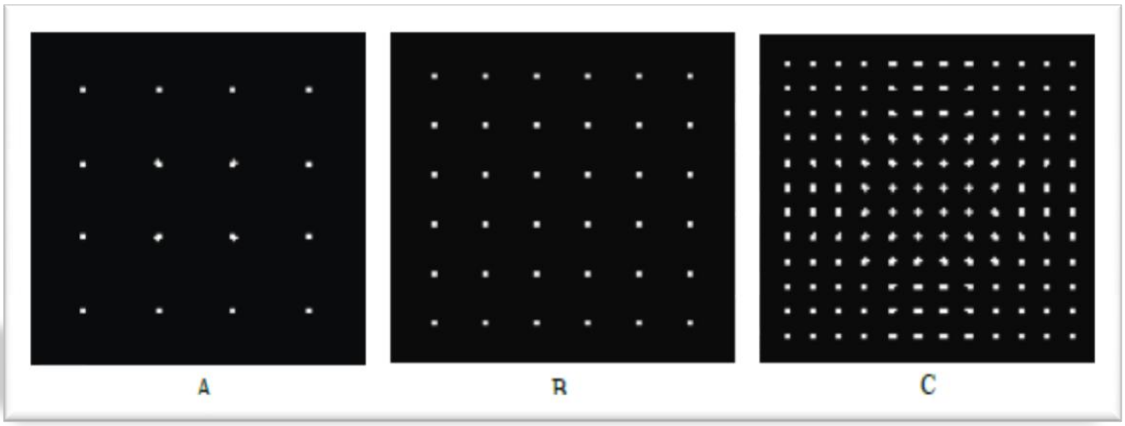

Figure 4. (A and B) The image reconstruction of SNRs before processing with DICOM, (C) Image reconstruction after processing with DICOM

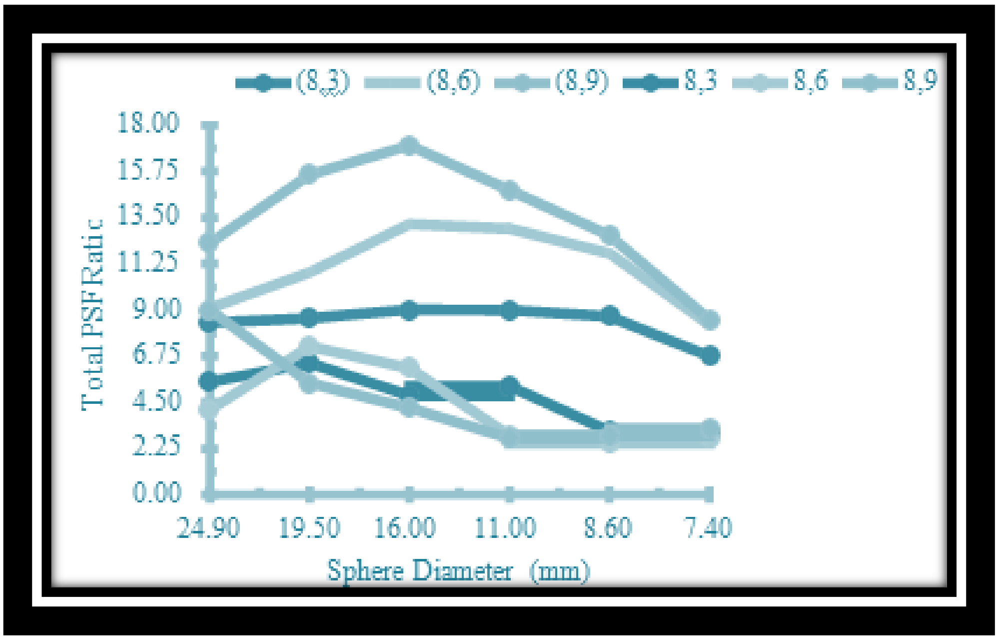

Figure 5. Relationship between SUV and PSF iteration number

International Innovative Research Journal of Engineering and Technology
ISSN: 2456-1983 Vol: 5 Issue: 2 December 2019

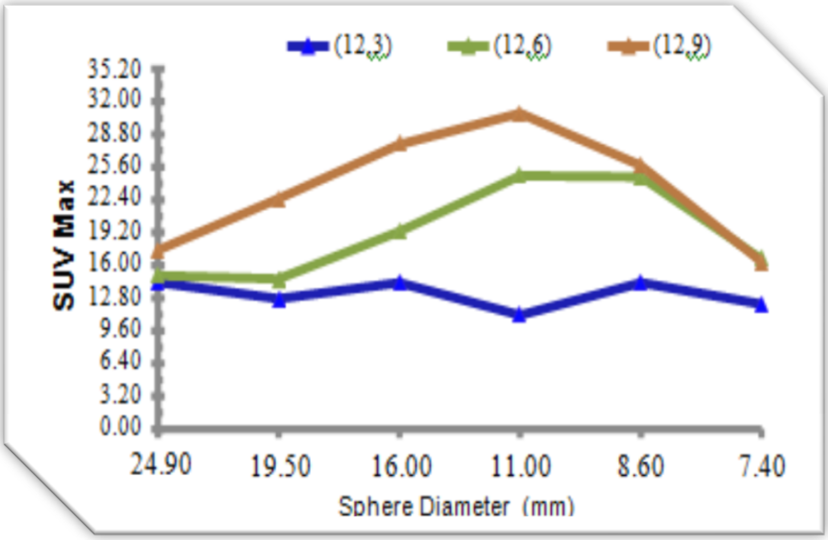

Figure 6. Relationship between total PSF ratio and standard sphere diameter without DICOM- MATLAB processing systems

The simulation consists of multiple parts: creating a virtual origin, modeling the response of the detector, and reconstruction of images [31]. However, the quantity efficiency and three SUV, PSF and SNR variables have been modelled into the simulation: intrinsic scintillator noise, dark and SiPM noise. First, the two-dimensional origin is generated by creating a large number of random events that represent the true locations of contact with the energy identified by the consumer. This determines the size of the detector and the structure of crystals. During imaging with Gamma lens, intrinsic scintillator noise occurs from electron trapping and thermally produced pairs of electron hole and used low-dose radioisotopes [32].

6. CONCLUSION

Of devices used in nuclear imaging, optimal performance and reliability should be extended to radiation safety standards and technological safety level specifications of methods and techniques during the imaging process. Used electrical circuit integration systems in Gamma camera machines improve and help image quality and promote image recovery.

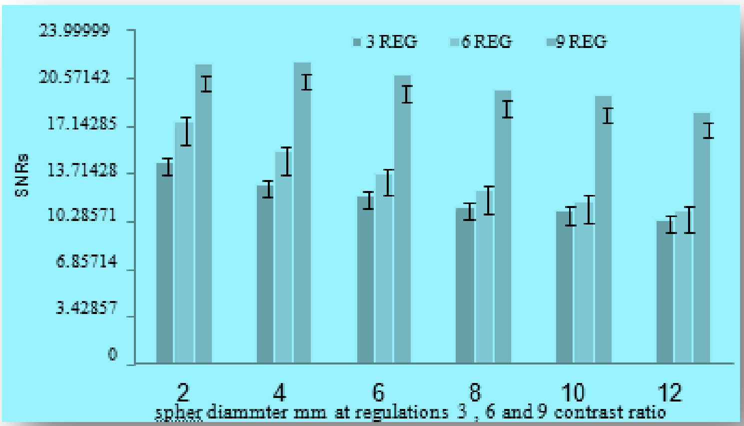

Figure 7. Relationship between total SUV MAX ratio and standard sphere diameter with DICOM- MATLAB processing systems

International Innovative Research Journal of Engineering and Technology
ISSN: 2456-1983 Vol: 5 Issue: 2 December 2019

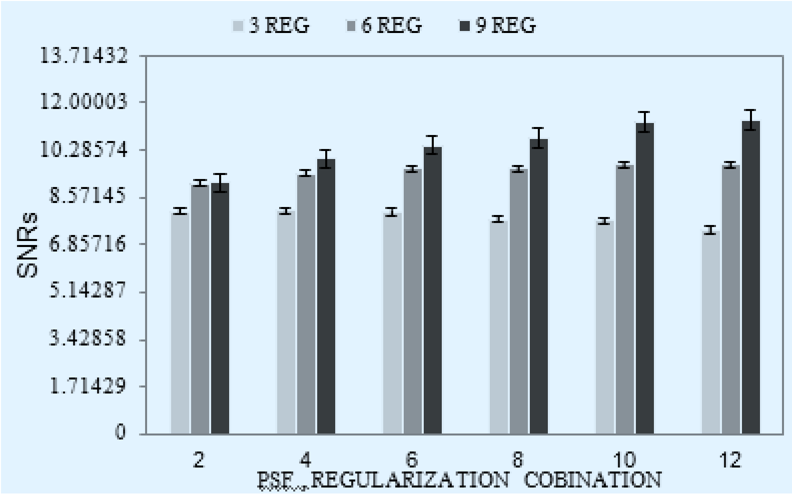

Figure 8. Relationship between sphere diameter and SNRs

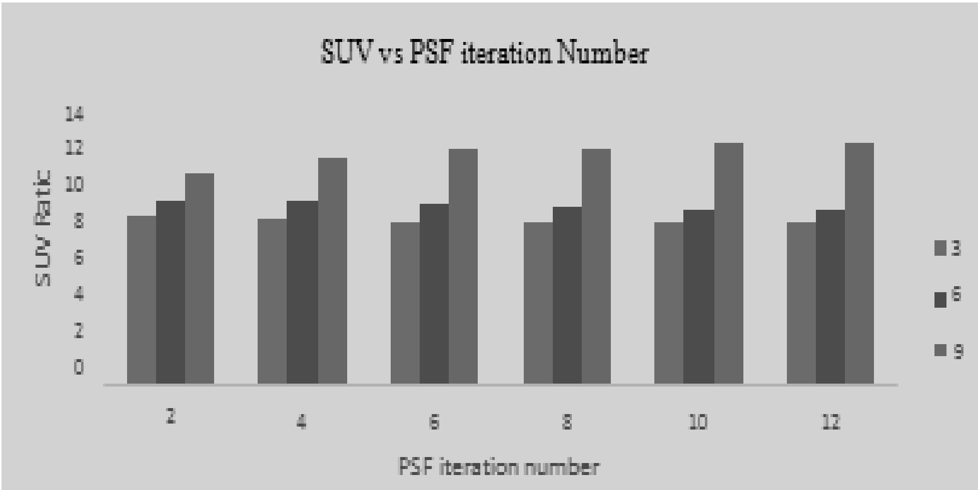

Figure 9. Relationship between SNRs and PSF

To use the neural intelligence systems DICOM – MATLAB, the imaging procedure and the radioisotopes used are protected by safety precautions and safety standards. The characteristics factors that influence image processing with Gamma camera SUV, PSF and SNRs, these factors play an important role in image processing to achieve high-quality image with low radioisotope dose.

REFERENCES

[1] AEA Safety Standards (2010) International Basic Safety Standards for Protection against Ionizing Radiation and for the Safety of Radiation Sources. IAEA Safety Series No: 115.

[2] National Electrical Manufacturers Association (NEM) (2001) A Performance Measurements of Scintillation Cameras. NEMA Standards Publication NU 1-2001, USA, Global Engineering Documents.

[3] Cerqueira MD, Allman KC, Ficaro EP, Hansen CL, Nichols KJ, et al. (2010) Recommendations for reducing radiation exposure in myocardial perfusion imaging. J Nucl Cardiol 17: 709-18.

[4] Costin H, Rotariu C (2002) Biomedical Image Analysis by Means of Soft- Computing and Semantic Networks. Proc. of EMBEC, Vienna Pp: 1574-1575.

[5] Costin H, Rotariu C (2003) Knowledge-Based Contour Detection in Medical Imaging Using Fuzzy Logic. Signals Circuits Sys Pp: 273-276.

International Innovative Research Journal of Engineering and Technology
ISSN: 2456-1983 Vol: 5 Issue: 2 December 2019

[6] Costin H (2004) Image Processing and Analysis. Applications in Biomedical Imaging. Tehnica Info Publ. House, Kisinev, Romanian.

[7] Costin H (2004) Biomedical Image Processing and Analysis via Artificial Intelligence and Information Fusion, Book Chapter in: Knowledge Based Intelligent Systems for Health Care, T. Ichimura and K. Yoshida (Eds.), Advanced Knowledge Int Publ Pp: 121-160.

[8] Yang YB, Chen SF (2018) Cell identification based on artificial neural network ensembles for gamma camera. Artificial Intelligence in Medicine 24: 25-36.

[9] Wells CP, Buxton-Thomas M (2016) Gamma camera purchasing. Nucl Med Commun 16: 168-185.

[10] Tindale WB (1995) Specifying dual detector gamma cameras and associated computer systems. Nucl Med Commun 16: 534-538.

[11] British Nuclear Medicine Society (2003) Gamma camera and data processor system tender questionnaire.

[12] Neau RE (2015) Non-uniformity energy correction method and apparatus.

[13] http://www.hamamatsu.com

[14] Kowalsky J, Falen SW (2013) Radiopharmaceuticals in Nuclear Pharmacy and Nuclear Medicine. J Nucl Med 54: 324-325.

[15] Lemaître C (2009) Use of machine learning algorithms for gamma detection in positron emission tomography. Vrije Universiteit Brussel.

[16] Arseneau RE (2016) Dynamic threshold for scintillation camera. INIS.

[17] Barfod JM (1990) Gamma camera with image uniformity byenergy correction offsets. US4899054A.

[18] Jeong MH, Choi Y, Chung YH, Song TY, Jung JH (2004) Performance improvement of small gamma camera using NaI(Tl) plate and position sensitive photo-multiplier tubes. Phys Med Biol 49: 4961.

[19] European Commission: Draft for updating Radiation Protection 91: Criteria for acceptability of radiological (including radiotherapy) and nuclear medicine Installations, FINAL DRAFT AMENDED-V1.4-091001 (EC, 2010).

[20] Busemann E (2010) Routine quality control recommendations for nuclear medicine instrumentation. Eur J Nucl Med Mol Imaging 37: 662-71.

[21] Hinton GE, Deng L, Yu D, Dahl GE, Mohamed AR (2012) Deep neural networks for acoustic modeling in speech recognition: The Shared Views of Four Research Groups. IEEE Signal Process Mag 29: 82-97.

[22] Masa-Ah P, Soongsathitanon S (2010) A Novel Standardized Uptake Value (SUV) Calculation of PET DICOM Files Using MATLAB. WSEAS Pp: 413-416.

[23] Masa-Ah P, Soongsathitanon S (2010) A Novel Scheme for Standardized Uptake Value (SUV) Calculation in PET Scans. Int J Math Models Methods Appl Sci 4: 291-299.

[24] Digital Imaging and Communication in Medicine (DICOM) (2016) Positron emission tomography image objects Supplement 64 ACR-NEMA.

[25] Hines H, Kayayan R, Colsher J, Hashimoto D, Schubert R, et al. (1999) Recommendations for implementing SPECT instrumentation quality control. EurJ Nucl Med 26: 527-532.

[26] Groch M, Erwin WD (2001) Single-photon emission computed tomography in the year 2001: instrumentation and quality control. J Nucl Med Technol 29: 12-8.

[27] Kanakatte A, Gubbi J, Mani N, Kron T, Binns D (2007) A Pilot Study of Automatic Lung Tumor Segmentation from Position Emission Tomography Images using Standard Uptake Values. Comput Intell in Image and Signal Process Pp: 363- 368.

[28] Novoa FJ, Castro AF, Pereira J, Pazos A (2004) Development of a DICOM server for the reception and storage of medical images in digital format. WSEAS Int Conf Appl Informatica and Commun.

[29] Pianykh OS (2008) Digital imaging and communications in medicine (DICOM): a practical introduction and survival guide. Berlin: Springer.

[30] Tararine M (1997) Method for correcting the uniformity of a gamma camera. US5606166A.